Acta Crystallographica Section B
Structural Science
ISSN 0108-7681

Different forms of antiparallel stacking of hydrogen-bonded antidromic rings in the solid state: polymorphism with virtually the same unit cell and two-dimensional isostructurality with alternating layers

Alajos Kálmán,[a]* László Fábián,[a] Gyula Argay,[a] Gábor Bernáth[b,c] and Zsuzsanna Cs. Gyarmati[c]

[a]Institute of Structural Chemistry, Chemical Reseach Center, Hungarian Academy of Sciences, PO Box 17, Budapest 114, H-1525, Hungary, [b]Research Group for Heterocyclic Chemistry, Hungarian Academy of Sciences and University of Szeged, Hungary, and [c]Institute of Pharmaceutical Chemistry, University of Szeged, PO Box 121, Szeged, H-6701, Hungary

Correspondence e-mail: akalman@chemres.hu

Received 27 July 2004
Accepted 30 September 2004

As a continuation of a systematic structural analysis of 2-hydroxycycloalkanecarboxylic acids and their carboxamide analogs, the effects of antidromic rings [Jeffrey & Saenger (1991). *Hydrogen Bonding in Biological Structures*. Berlin, Heidelberg: Springer Verlag] upon the layer stacking of cyclopentane and cycloheptane derivatives are compared. Determination of the structure of *trans*-2-hydroxycycloheptanecarboxylic acid (2) led to the discovery of two polymorphs with virtually the same unit cell [Kálmán *et al.* (2003). *J. Am. Chem. Soc.* **125**, 34–35]. (i) The layer stacking of the antidromic rings for the whole single crystal is antiparallel (2*b*). (ii) The antidromic rings and the 2_1 axis are parallel (2*a*), consequently the domains of the single crystal must be antiparallel. While their polymorphism is solvent-controlled, they illustrate a novel form of two-dimensional isostructurality. Antiparallel layer stacking is again demonstrated by *trans*-2-hydroxycycloheptanecarboxamide (3) (space group *Pbca*). It is built up from layers isostructural with those in the homologous *trans*-2-hydroxycyclopentanecarboxamide (4) [Kálmán *et al.* (2001). *Acta Cryst.* B**57**, 539–550], but in this structure (space group $Pca2_1$) the layers are stacked in parallel mode. Similar to (2*a*) and (2*b*), the antiparallel layer stacking in (3) *versus* their parallel array in (4) illustrates the two-dimensional isostructurality with alternating layer orientations. Although (3) and (4) display isostructurality, they are not isomorphous.

1. Introduction

Among the crystal structures of several alicyclic 2-hydroxycarboxylic acids (Kálmán *et al.*, 2001, 2002*a*,*b*) formed by either lateral or linear associations of molecular dimers described by the graph-set motif $R_2^2(12)$ (Etter, 1990; Bernstein *et al.*, 1995), (1*R**,2*S**,5*R**)-5-*tert*-butyl-2-hydroxycyclopentanecarboxylic acid [(1), *cf.* Fig. 1] exhibits a different form of close packing. Four molecules, related by a glide plane *n*, link up to produce a large $R_4^4(18)$ ring (Kálmán *et al.*, 2001). These rings, held together by O—H···O=C and O—H···O(H) hydrogen bonds, are antidromic rings (see *Appendix A*), which Jeffrey & Saenger (1991) consider to have a significant total dipole moment. Jeffrey and Saenger claimed that 'macroscopically, the dipoles must cancel for the whole crystals, either by antiparallel arrangements in the crystal unit cell or by antiparallel alignment of domains in the crystals'. In (1) this condition is satisfied by antiparallel layer stacking governed by centers of symmetry with the space group $P2_1/n$ (Kálmán *et al.*, 2001). We have previously demonstrated (Kálmán *et al.*, 2003) that the supramolecular self-organization pattern found in (1) (Kálmán *et al.*, 2002*a*) may have two other

forms of layer stacking. A serendipitous (Merton & Barber, 2004) crystallization of *trans*-2-hydroxycycloheptanecarboxylic acid (2) led to the discovery of these close-packing forms as a previously unrecognized form of polymorphism (Bernstein, 2002). The crystals obtained both from dibutyl ether (2*a*) and diethyl ether (2*b*) exhibited virtually the same unit cell. However, the sequences of their space-group symmetries are different: $Pna2_1$ or $Pn2_1a$,[1] which can be attributed to antiparallel (2*b*) or parallel (2*a*) layer stacking. The common feature of (1), (2*a*) and (2*b*) is the presence of antidromic rings (Fig. 2), denoted by the graph-set motif $R_4^4(18)$ with three different forms (*a*, *b* and *c*) of 'antiparallel' stacking depicted in Fig. 3.

The recent structure determination of *trans*-2-hydroxycycloheptanecarboxamide [hereinafter (3)] again demonstrated an antiparallel stacking of polar layers *via* centers of symmetry (form *a*). Similar polar layers had earlier been found in the cyclopentane homolog of (3) [*trans*-2-hydroxycyclopentanecarboxamide, hereinafter (4)], but they are stacked in a parallel mode (Kálmán *et al.*, 2001). How can this marked difference in the stacking mode be explained? Since (3) is also the carboxamide derivative of (2), a comparison of the layer structure of (2) *versus* (3) enabled us to see how the third type of hydrogen bond (N—H···O═C) reorganizes the polar layers which are formed exclusively by antidromic rings in (1), (2*a*) and (2*b*).

Analysis of the similarities and differences in the stacking modes of the layer structures in the crystals of the four related compounds (Fig. 1) revealed:

(*a*) the solvent-controlled polymorphism of (2) and, in contrast,

(*b*) the stability of the centrosymmetric crystals of (3) (space group *Pbca*) and the polar crystals of (4) (space group $Pca2_1$) in different solvents and in response to heating.

Analysis of the parallel *versus* antiparallel stacking modes in the dimorphic (2*a*) and (2*b*), and the homologous (4) and (3) additionally revealed a new form of isostructurality (Kálmán *et al.*, 1993; Kálmán & Párkányi, 1997; Fábián & Kálmán, 1999).

2. Experimental

2.1. Synthesis

The synthesis of *trans*-2-hydroxycycloheptanecarboxamide (3) has been previously reported (Bernáth *et al.*, 1973). Similarly, as for the cyclopentane homolog (Bernáth *et al.*, 1972), a solution of *trans*-2-carbethoxycycloheptanol in absolute methanol saturated with ammonia was allowed to stand at room temperature for 10 d. The product (3) remaining after evaporation of the methanol was recrystallized twice from benzene to obtain white crystal plates with m.p. 400–401 K.

[1] If we label the orthorhombic cell vectors in the decreasing sequence $a > b > c$ for both (2*a*) and (2*b*) phases, then the canonical space-group notation $Pna2_1$ (2*a*) should be transformed into the non-standard form $Pn2_1a$ (2*b*).

2.2. Data collection, structure solution and refinement

To check on possible solvent effects [*e.g.* a polymorphism similar to that for the parent compound (2)], X-ray quality crystals of (3) were obtained from ethanol and diethyl ether and data sets were collected on both at room temperature on a CAD-4 diffractometer equipped with a graphite monochromator; the two crystals proved to have the same structure. The structure determined for the crystal obtained from diethyl

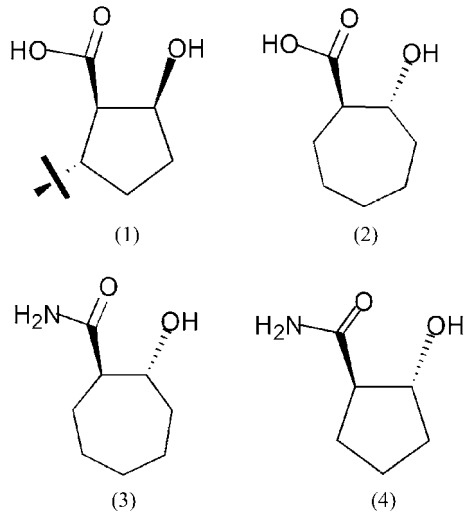

Figure 1
Chemical structures of (1*R**,2*S**,5*R**)-5-*tert*-butyl-2-hydroxycyclopentanecarboxylic acid (1), *trans*-2-hydroxycycloheptanecarboxylic acid (2), *trans*-2-hydroxycycloheptanecarboxamide (3) and *trans*-2-hydroxycyclopentanecarboxamide (4).

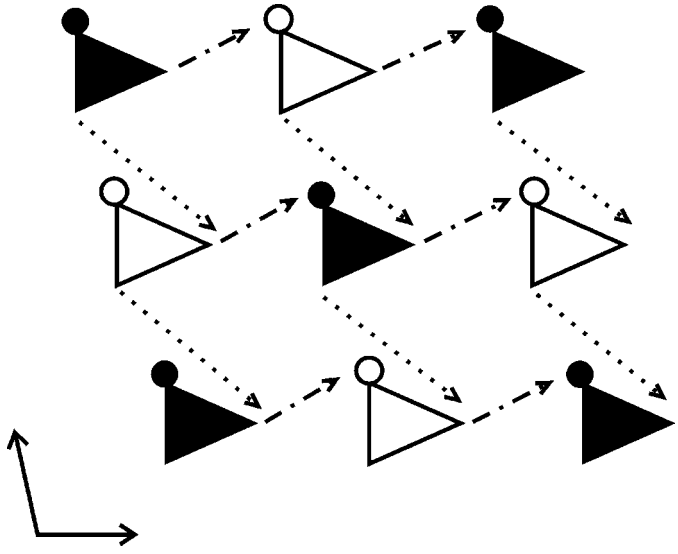

Figure 2
Symbolic presentation of the close-packing pattern with heterochiral chains in a parallel array. The alicyclic rings are omitted. The black and white triangles differentiate the enantiomers, while the points (two) represent the OH groups and the small circle denotes the CO moiety. Two white and two black triangles in a diagonal array, generated by a glide plane *n*, produce the antidromic $R_4^4(18)$ rings. The possible stacking modes of such a layer: (*a*), (*b*) and (*c*) are shown in Fig. 3.

Table 1
Experimental details.

Crystal data	
Chemical formula	$C_8H_{15}NO_2$
M_r	157.21
Cell setting, space group	Orthorhombic, *Pbca*
a, b, c (Å)	8.248 (1), 19.679 (3), 10.581 (1)
V (Å^3)	1717.4 (4)
Z	8
D_x (Mg m^{-3})	1.216
Radiation type	Mo $K\alpha$
No. of reflections for cell parameters	25
θ range (°)	15.4–17.2
μ (mm^{-1})	0.09
Temperature (K)	293 (2)
Crystal form, color	Prism, colorless
Crystal size (mm)	0.55 × 0.50 × 0.20
Data collection	
Diffractometer	Enraf–Nonius CAD-4
Data collection method	ω–2θ
Absorption correction	φ scan
T_{min}	0.875
T_{max}	0.980
No. of measured, independent and observed reflections	6109, 2969, 1666
Criterion for observed reflections	$I > 2\sigma(I)$
R_{int}	0.022
θ_{max} (°)	32.0
Range of h, k, l	$-12 \Rightarrow h \Rightarrow 12$ $-29 \Rightarrow k \Rightarrow 29$ $-15 \Rightarrow l \Rightarrow 15$
No. and frequency of standard reflections	3 every 60 min
Intensity decay (%)	5
Refinement	
Refinement on	F^2
$R[F^2 > 2\sigma(F^2)]$, $wR(F^2)$, S	0.045, 0.145, 0.85
No. of reflections	2969
No. of parameters	101
H-atom treatment	Riding
Weighting scheme	$w = 1/[\sigma^2(F_o^2) + (0.1P)^2]$, where $P = (F_o^2 + 2F_c^2)/3$
$(\Delta/\sigma)_{max}$	<0.0001
$\Delta\rho_{max}$, $\Delta\rho_{min}$ (e Å^{-3})	0.30, −0.20

Computer programs: *CAD*-4 *Express* (Enraf–Nonius, 1992), *XCAD*-4 (Harms, 1996), *SHELXS*97 (Sheldrick, 1997*a*), *SHELXL*97 (Sheldrick, 1997*b*).

ether is presented here. Three standard reflections (measured every 60 min) indicated some crystal decay (5%); consequently, the reflections were corrected by means of the program *XCAD*-4 (Harms, 1996). All reflections were corrected for Lorenz and polarization effects. The space group *Pbca* was determined from the unit-cell volume, symmetry and systematic absences. The crystallographic phase problems were solved by direct methods, using the program *SHELXS*97 (Sheldrick, 1997*a*). The atomic positions were refined with anisotropic displacement parameters on F^2, with the program *SHELXL*97 (Sheldrick, 1997*b*). The positions of the H atoms bound to O and N atoms were located in difference-Fourier maps, while the others were generated from the assumed geometry and were refined isotropically in the riding mode (Table 1).[2] For comparison, the lattice parameters of the structures (2*a*), (2*b*), (3) and (4) are listed in Table 2.

2.3. Powder patterns

For each crystal structure determined by the single-crystal technique [(2*a*), (2*b*), (3) and (4)], powder patterns were generated by the programs *LAZY PULVERIX* (Yvon *et al.*, 1977) and *PLATON* (Spek, 1998). Powder patterns of the polymorphs of (2) crystallized from diethyl ether (2*b*) and dibutyl ether (2*a*), their 1:1 mixture, diisopropyl ether and benzene were produced with monochromated Cu $K\alpha$ radiation on a vertical high-angle Philips PW 1050 powder diffractometer. Powders of (3) and (4), crystallized from different solvents, were characterized similarly. The effect of preferred orientation, displayed in particular by the recrystallized samples of (2*a*) and (2*b*), was diminished by vigorous pulverization in an agate mortar. Differential thermal analysis (DTA) of (2*a*), (2*b*) and (4) was performed with a MOM (Budapest) 2-1500D derivatograph.

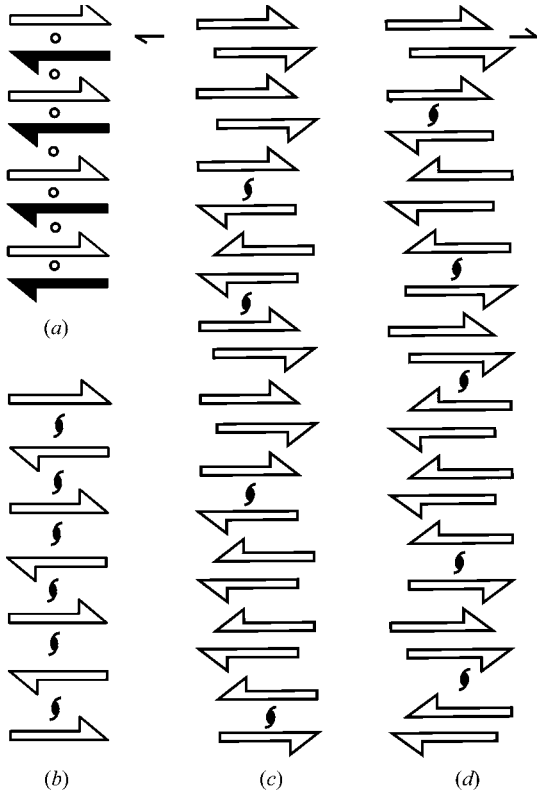

Figure 3
Modeling of the three modes of layer stacking. Each arrow (black or white) represents a heterochiral layer of $R_4^4(18)$ tetramers. (*a*) In (1) antiparallel layer stacking is formed *via* centers of symmetry. (*b*) In (2*b*) the layers are antiparallel *via* the screw axes which are perpendicular to the dipole vectors. (*c*) In (2*a*) the layers are parallel *via* the screw axes (indicated by a slight shift between the arrows), which are parallel to the dipole vectors. The domains formed by parallel layers are stacked upon each other in an antiparallel mode. Consequently, each boundary (shown by the 'perpendicular' screw axis) between the antiparallel domains is a double layer of (2*b*). (*d*) With an increasing number of boundaries the quality of the (2*a*) crystals diminishes.

[2] Supplementary data for this paper are available from the IUCr electronic archives (Reference: DE5011). Services for accessing these data are described at the back of the journal.

Table 2
Crystal data on (2*a*) and (2*b*) and the carboxamides (3) and (4).

Crystal	*a* (Å)	*b* (Å)	*c* (Å)	*V* (Å^3)	Density (Mg m^{-3})	Space group
(2*a*)	21.184 (3)	6.824 (1)	5.892 (2)	851.7 (3)	1.234	$Pna2_1$
(2*b*)	21.185 (2)	6.826 (1)	5.889 (1)	851.6 (2)	1.234	$Pn2_1a$
(3)	8.248 (1)	19.679 (3)	10.581 (1)	1717.4 (4)	1.216	*Pbca*
(4)†	8.250 (2)	8.410 (2)	9.879 (2)	685.4 (3)	1.252	$P2_1ca$

† For a straightforward comparison of the lattice parameters of (3) and (4), the *a* and *c* axes are interchanged. Consequently, the standard space group setting of $Pca2_1$ is replaced with $P2_1ca$.

3. Results and discussion

3.1. Layer and domain stacking in the carboxylic acids (1), (2*a*) and (2*b*)

In our preliminary report on the polymorphism of (2) (Kálmán *et al.*, 2003), we demonstrated the nearly identical puckerings of the $R_4^4(18)$ rings in the (2*a*) and (2*b*) phases. In both crystals the overall dipole of the antidromic rings (Jeffrey & Saenger, 1991) points in the direction of the *c* axis. We showed that the close-packed layer pattern of heterochiral chains in a parallel array (Fig. 2) may be rotated around the three crystal axes to give the three different stacking modes (*a*), (*b*) and (*c*) depicted in Fig. 3. In (1) the antiparallel layers are held together by centers of inversion (*a*), whereas in the dimorphs of (2) (Table 2) the layers are related by screw axes located between the parallel layers. In the unit cell of (2*b*) (space group $Pn2_1a$) the screw axis is perpendicular to the dipole vector (*b*), whereas in (2*a*) (space group $Pna2_1$), it is parallel (*c*) to the dipole vector. In the latter case, the ring dipoles remain parallel. Their mandatory antiparallel alignment in (2*a*) is provided by domains, as predicted for such a case by Jeffrey & Saenger (1991). As depicted in Figs. 4 and 5 in the preliminary paper (Kálmán *et al.*, 2003), the upper halves of the unit cells are identical. In the lower halves, the mutually perpendicular 2_1 rotations (around the *b* and *c* axes, respectively) are related by a twofold axis which, by a 180° turn of one of the unit cells around the *a* axis, makes the lower halves identical. Consequently, (2*a*) and (2*b*), with virtually identical unit-cell parameters, illustrate a novel form of isostructurality. They exhibit two-dimensional isostructurality (Fábián & Kálmán, 2004) with alternating layer orientations (Figs. 3*b* and *c*). The adjacent layers of each domain in (2*a*) are held together by weak van der Waals forces. Such domains with variable thickness (Figs. 3*c* and *d*) are stacked upon each other in an antiparallel sequence. Since each boundary between the antiparallel domains is a double layer of (2*b*), the domains of (2*a*) unavoidably contain (2*b*) layers in random sequence. Consequently, a pure form of (2*a*) cannot be isolated and the amount of (2*b*) in (2*a*) may vary from crystal to crystal (Figs. 3*c* and *d*).

3.2. Layer stacking in the carboxamides (3) and (4)

In the close packing of (3), similar to that in (4), each molecular tetramer forms three antidromic rings with the graph-set motifs $R_4^3(12)$, $R_4^3(18)$ and $R_4^4(22)$, which are accompanied by a homodromic $R_4^4(18)$ ring. For a better view, the four rings are shown separately in a schematic view of the layer packing (Fig. 4). The common helical backbones are held together by the O—H···O═C bonds inherited from the carboxylic acid (2). The N—H···O═C hydrogen bond either alone (in pairs) or together with the N—H···O(H) bonds, which replace the O—H···O(H) bonds of the carboxylic acid(s), furnish the three antidromic rings. The O—H···O═C and the N—H···O═C hydrogen bonds yield the symmetric $R_4^3(18)$ ring, whereas the asymmetric $R_4^3(12)$ and $R_4^4(22)$ rings are formed through the participation of all three types of hydrogen bond. In contrast, the homodromic $R_4^4(18)$ ring is formed by the O—H···O═C and N—H···O(H) bonds. Consequently, the total dipole effect seems to be weakened by the different orientations (and magnitudes) of the dipoles generated in the $R_4^3(18)$, $R_4^3(12)$ and $R_4^4(22)$ rings and buffered by the homodromic $R_4^4(18)$ ring. This is why the antiparallel layer stacking of (3) cannot be attributed conclusively to the antidromic ring effect, as was possible in the cases of (1), (2*a*) and (2*b*). The parallel stacking found in (4) supports this conclusion.

Nevertheless, apart from the sizes of the alicyclic rings, the layer structures of (4) and (3) (Fig. 5) are rather similar. The layers of hydrogen-bonded helices in (4) are parallel, whereas the helices in the homologous cycloheptane derivative (3) are antiparallel (Fig. 6); consequently, this is a second case of alternating two-dimensional isostructurality, recognized previously between (2*a*) and (2*b*). It gives rise to a doubled *b* axis in (3) compared with that in (4) (Table 2) and within this distance every second layer is isostructural with the corre-

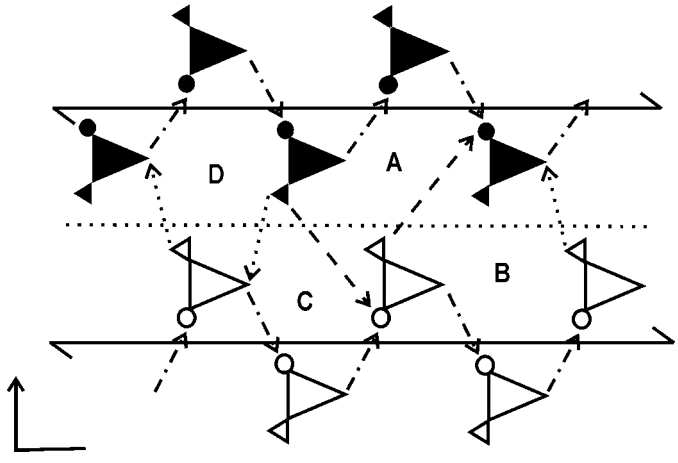

Figure 4
Separate symbolic presentation of the common rings in the layer structures of (3) and (4). The symbols are the same as given in Fig. 2 and the ring constitutions are described in Table 3. The five- and seven-membered rings are omitted, while the small triangles represent the amino groups. The antidromic $R_4^3(18)$ (*A*), $R_4^4(22)$ (*B*) and $R_4^3(12)$ (*C*) rings are closed by N—H···O═C hydrogen bonds and exhibit different dipole vectors in magnitude and direction. The O—H···O═C and N—H···O(H) hydrogen bonds form a homodromic $R_4^4(18)$ (*D*) ring.

Table 3
Graph-set notations $R_d^a(n)$ of the four tetrameric rings observed in the layer structures of (3) and (4) (Fig. 3).

They are partitioned in terms of the ring components ${}_dC^a$ (Kálmán *et al.*, 2001). The arrows indicate the donor ⇒ acceptor directions which determine the antidromic and homodromic characters of the rings.

$R_4^3(18)$: $\leftarrow {}_27^0 \rightarrow {}_16^1 \rightarrow {}_01^1 \leftarrow {}_14^1 \leftarrow$ antidromic (*A*)
$R_4^4(22)$: $\leftarrow {}_27^0 \rightarrow {}_16^1 \rightarrow {}_14^1 \rightarrow {}_05^2 \leftarrow$ antidromic (*B*)
$R_4^3(12)$: $\rightarrow {}_12^1 \rightarrow {}_16^1 \rightarrow {}_01^1 \leftarrow {}_23^0 \rightarrow$ antidromic (*C*)
$R_4^4(18)$: $\rightarrow {}_16^1 \rightarrow {}_12^1 \rightarrow {}_16^1 \rightarrow {}_14^1 \rightarrow$ homodromic (*D*)

sponding (say 'even') unit cell of (4). At the same time, the 'odd' layers in (3) and the 'odd' unit cells of (4) exhibit isostructurality *via* inversion.

3.3. Solvent-dependent polymorphism of (2)

Since the polymorphism of (2) has an impact on the powder patterns of (2*a*) and (2*b*), they could be used to study the solvent dependence of the layer stacking discussed above. The patterns computed from the atomic coordinates of (2*a*) and (2*b*) are depicted in Fig. 7. While the Bragg angles (θ) of the reflections are the same, their intensities at several d values differ considerably. In particular, the 301, 111, 020, 220, 420 and 412 reflections are much stronger in the powder pattern of (2*b*) than in that of (2*a*). In contrast, the 401, 120, 510 and 312 reflections display greater intensities in the pattern of (2*a*) than in that of (2*b*).

A powder crystallized from dibutyl ether gave an X-ray pattern (Fig. 8*a*) which coincided essentially with the computed intensities of (2*a*) (Fig. 7*a*). Similarly, the pattern obtained from the pulverized sample crystallized from butan-2-one agreed with the computed diffractogram of (2*b*), although the pattern was strongly influenced by the preferred orientation of the particles. The pattern of (2*b*) (Fig. 8*b*), which was less strongly affected by the preferred orientation, was repeatedly obtained from diethyl ether. Since both polymorphs could be obtained without visible impurities from two ether solvents, the effect of the length of the alkyl chains on the polymorphism was tested with diisopropyl ether. On recrystallization from diisopropyl ether (Fig. 8*c*), solutions of both (2*a*) and (2*b*) furnished (2*b*) containing a small amount of (2*a*) (Bernstein, 2002). Recrystallization of pure (2*a*) and (2*b*) from a 1:1 mixture of dibutyl ether and diethyl ether afforded large flakes, which exhibited a preferred orientation even after vigorous pulverization. Nevertheless, one of the samples was predominantly (2*b*) with a small amount of (2*a*), whereas the other sample was (2*a*) which was free from (2*b*). It follows that, depending on the cooling, concentration *etc.*, a 1:1 mixture of diethyl ether and dibutyl ether as the solvent does not hinder the predominant crystallization of either polymorph. However, the X-ray pattern of the sample (Fig. 8*e*) obtained from a 1:1:1 mixture of diethyl and dibutyl ethers and butan-2-one, also affected by the preferred orientation, revealed that this mixture is inappropriate for the formation of the domain structure of (2*a*).

In an earlier description of (2) (Palau *et al.*, 1964) the crude material was purified by recrystallization from benzene. Accordingly, we recrystallized a small amount of the original product (2) from benzene; it proved to be (2*b*). Recrystallization from benzene was then repeated on the samples obtained from dibutyl ether (2*a*) and diethyl ether (2*b*). Both samples displayed a preferred orientation of the particles and gave the powder patterns of (2*b*) (Fig. 8*d*). This suggests that the formation of pure or mixed (2*a*) or (2*b*) depends on the length of the alkyl chains and/or the overall size of the solvent molecule. Thus, (2*a*), with its structure stabilized by antiparallel domains, was obtained only from dibutyl ether, with the longest alkyl chains (Fig. 9), whereas the pure form of (2*b*) was formed from diethyl ether and the analogous butan-2-one,

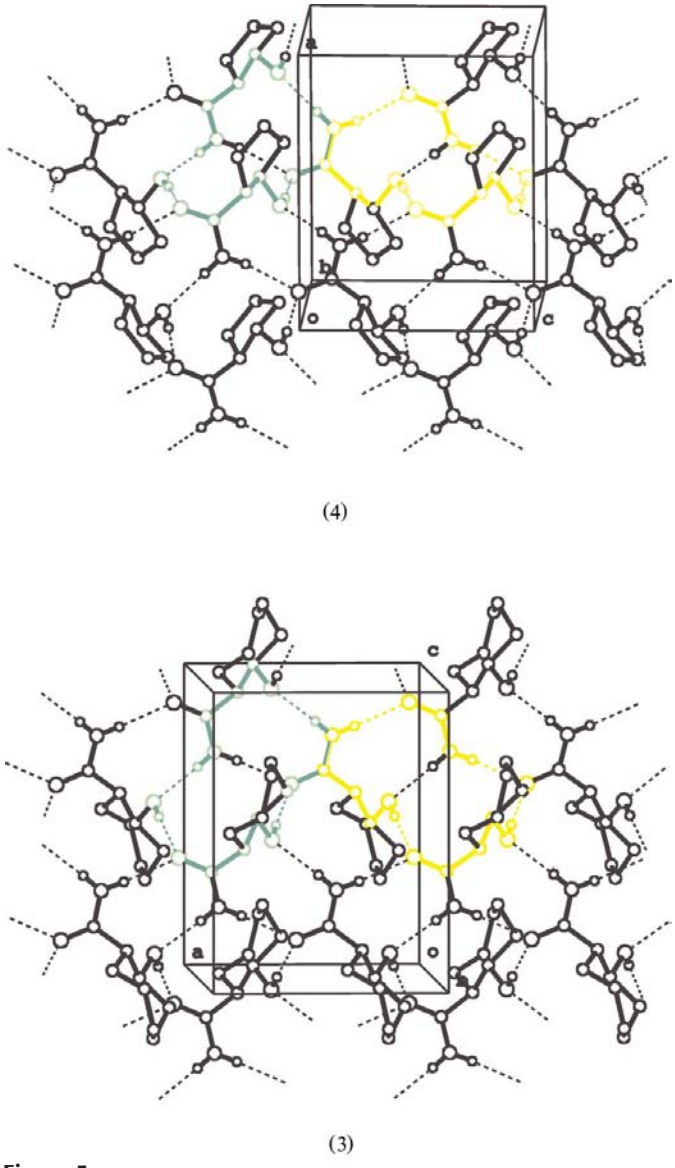

Figure 5
Perspective view of the polar molecular layers of (4) and (3) formed on the parallel helices along the *b* axis. The 18-membered homodromic (left) and antidromic (right) rings are shown in different colors. Apart from the five- and seven-membered rings, the patterns can hardly be distinguished from each other.

with short alkyl chains, and from the compact benzene. In the course of the crystallization of (2) from different solvents, no other crystal form was detected.

In contrast, neither the polymorphism of (3) nor a $P2_1ca \rightarrow Pbca$ phase transition of (4) was observed in the tested solvent mixtures. While (4) is insoluble in apolar solvents such as benzene, it yields the same form from a 1:4 mixture of 2-propanol and *n*-hexane, and a 2:1 mixture of ethanol and *n*-hexane.

3.4. Thermal investigations

An earlier investigation of (1) (Riddell *et al.*, 1995) by single-crystal X-ray diffraction, powder diffraction and solid-state NMR revealed three polymorphs. One of them was obtained by heating (1) for 20 min at 363 K. Its powder pattern indicated a novel phase, but its structure could not be determined. When molten (1) was allowed to cool to ambient temperature, the material obtained provided NMR evidence of the existence of a third phase containing a small amount of the second phase. The reported polymorphism of (1) suggests the second [represented by (2*b*)] and the third [represented by (2a)] stacking modes of dipole extinction. In an attempt to find similar phase transitions, possibly in favor of the first stacking mode [represented by (1)], (2*a*) and (2*b*) were subjected to thermal investigation. According to McCrone (1965), polymorphs may interconvert, but do not necessarily do so, in at least one direction, without going through the melt. In our case, no such phenomenon was observed. Up to their melting points [362.5 K for (2*a*) and 363 K for (2*b*)] no phase transition occurred and up to 398 K neither endothermic nor exothermic peaks were observed. The energetic equivalence of the forms (2*a*) and (2*b*), substantiated by the DTA curves, is in accordance with their cocrystallization, as discussed above.

No phase transition of (4) was observed either on DTA below the melting point of 375 K nor when the melt was heated up to 403 K. This suggests the stability of (4) with its polar space group against dipole effects and leaves its special relationship with (3) in the realm of alternating two-dimensional isostructurality.

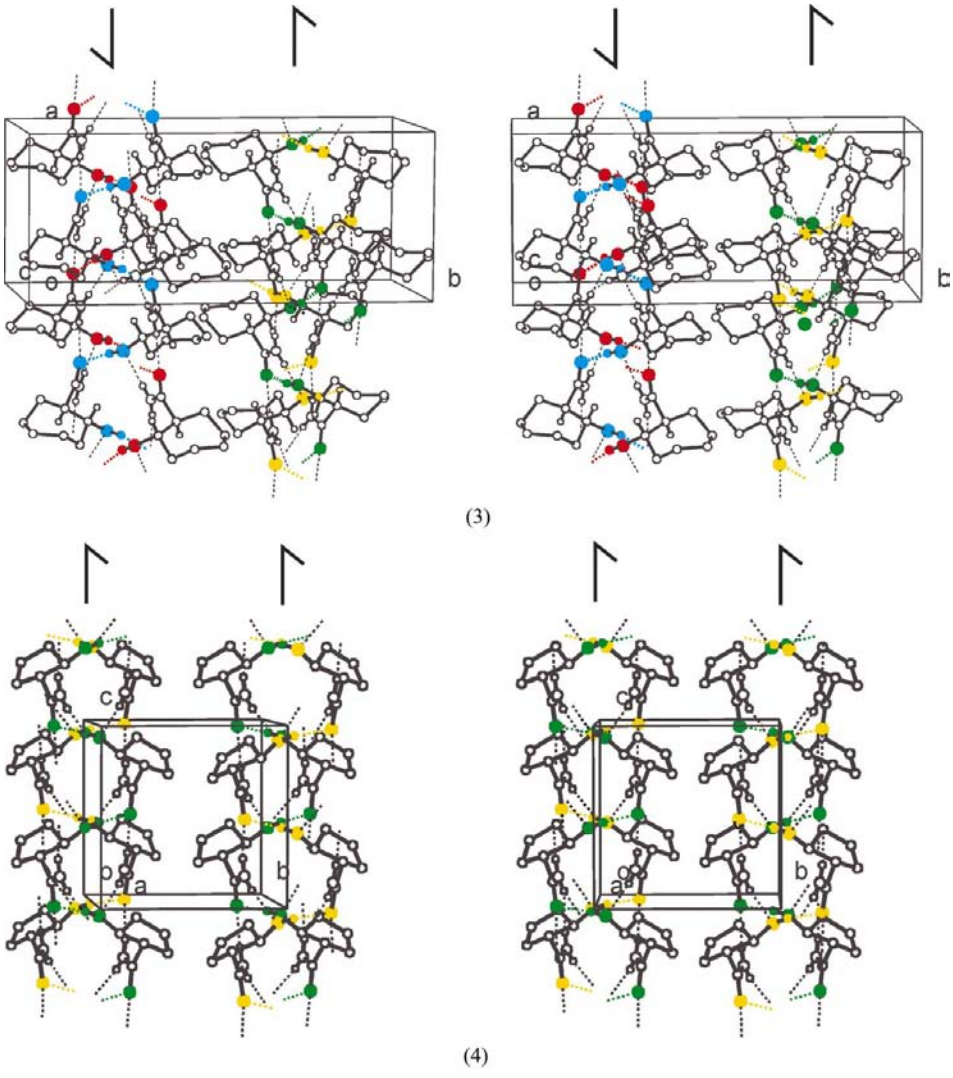

Figure 6
Stereoview of the close packing of (3) and (4). The alternate two-dimensional isostructurality is revealed by the antiparallel helices in (3) *versus* the parallel helices in (4). In both structures the enantiomers denoted by 4*R* are held together by the hydrogen bonds shown in green, whereas the helices with a 4*S* configuration are shown by yellow hydrogen bonds. The antiparallel double helix in (3) is indicated in blue (4*R*) and red (4*S*).

4. Conclusions

The study of the polymorphism of (2) (Kálmán *et al.*, 2003) has been extended to its solvent-dependent crystallization, which affords both pure and coexisting forms of the dimorphs (2*a*) and (2*b*). Their thermal investigations did not reveal a phase transition in either direction. The principal difference between (2*a*) and (2*b*) is their opposite modes of dipole extinction. While the dipoles generated in *trans*-2-hydroxycycloheptanecarboxylic acid molecules are canceled out by antiparallel layer stacking in (2*b*), the dipole extinction in (2*a*) is achieved by antiparallel crystal domains. Consequently, within a domain in (2*a*) the antidromic layers (the

'odd' or 'even' halves of the unit cell along the polar axis) are parallel, while in the unit cells of (2*b*) they are antiparallel. The polymorphs of (2) and an X-ray quality single crystal of one of the polymorphs of (1) exemplify the three canonical forms of dipole extinction generated by strong antidromic effects.

The dipole effects, balanced by the presence of one homo- and three antidromic rings with different orientations, cannot play a decisive role in the stacking mode in (3) and (4), and this accounts for their two-dimensional isostructurality. The polar layers of (3) are ordered in antiparallel stacking *via* inversion, while in (4) the 'same' layers remain parallel. This two-dimensional isostructurality is shown directly by the $2n \pm 1$ layers and unit cells with the same orientation. Apart from the different arrangements of the layers (*a*) parallel to or (*b*) perpendicular to the polar axes, the antiparallel layer stacking of (3) *via* inversion resembles that present in (1).

These examples of isostructurality cannot be described in terms of the isomorphism recognized by Mitscherlich in 1819.

(*a*) At a macroscopic level, the crystal habits of (2*a*) and (2*b*) differ, while their unit cells are the same.

(*b*) While the isostructurality of the crystals of (3) and (4) is obvious, with the doubled unit cell along the *b* axis, (3) cannot be regarded as isomorphous with (4).

It follows that the word 'isomorphic' is insufficient to describe the structural similarities between organic crystals. As suggested earlier (Kálmán & Párkányi, 1997), crystal isomorphism, as a classical 'morphological' term, should be distinguished from isostructurality.

Finally, once more on the role of serendipity. If by chance (2) had first been crystallized for X-ray studies from one of the common solvents such as diethyl ether, benzene or butan-2-one instead of dibutyl ether, we would not have tried to obtain better crystals, which turned out to be (2*b*) with the alternative of antiparallel layer stacking. The possibility of dipole extinction *via* domain stacking would have remained pure speculation (Jeffrey & Saenger, 1991).

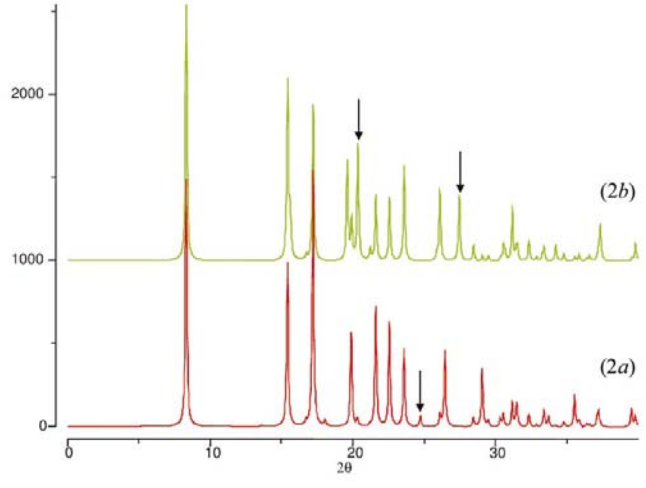

Figure 7
X-ray powder patterns of (2*a*) and (2*b*), calculated from the atomic coordinates obtained from single crystal studies with the program *PLATON* (Spek, 1998). Arrows indicate the noteworthy differences in intensity of the same reflections.

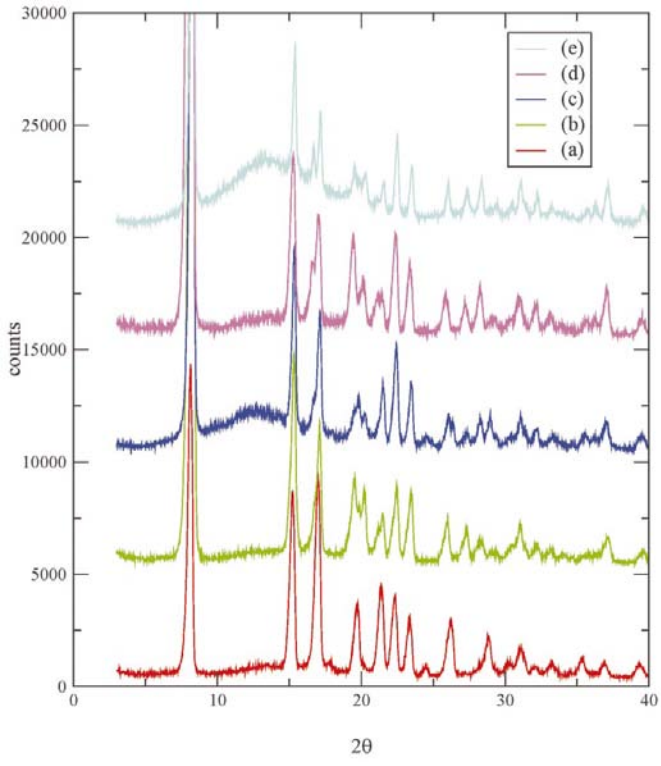

Figure 8
Solvent dependence of the polymorphism of (2) as revealed by X-ray powder patterns: (*a*) (2*a*) crystallized from dibutyl ether, (*b*) (2*b*) crystallized from diethyl ether, (*c*) (2*b*) crystallized together with (2*a*) from diisopropyl ether, (*d*) (2*b*) obtained from benzene and (*e*) (2*b*) obtained from a 1:1:1 mixture of diethyl ether, butan-2-one and dibutyl ether.

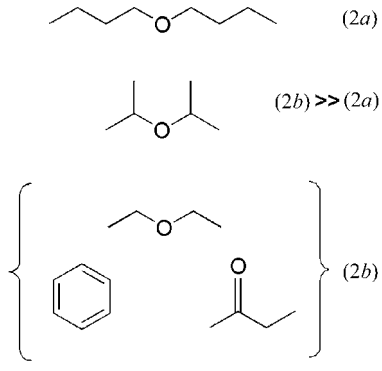

Figure 9
The solvents applied in the study of the polymorphism of (2*a*) and (2*b*). From the top downwards: dibutyl ether, diisopropyl ether, diethyl ether, benzene and butan-2-one.

APPENDIX *A*
The definition of the homo-, hetero- and antidromic rings formed by hydrogen bonds of O—H···O type

In the book '*Hydrogen Bonding in Biological Structures*' (1991, p. 38) Jeffrey and Saenger defined the homodromic (*A*), antidromic (*B*) and heterodromic (*C*) rings for cyclodextrin hydrates as shown below. These definitions for pentamers have been adapted for the tetramers observed in the structures discussed here.

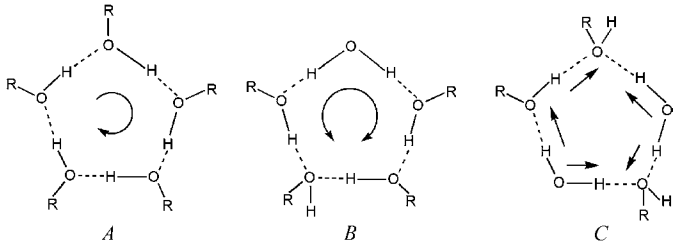

A *B* *C*

We thank Mr Csaba Kertész for the X-ray measurements, and Mrs Gy. Tóth-Csákvári, Mrs E. Dinya-Juhász, Mrs Ágnes Wellisch and Ms Nikoletta Báthori for their assistance. This work was supported by Hungarian Research Fund (OTKA) grants T03499985, T030547 and T034422.

References

Bernáth, G., Göndös, Gy., Kovács, K. & Sohár, P. (1973). *Tetrahedron*, **29**, 981–984.
Bernáth, G., Láng, K. L., Göndös, Gy., Márai, P. & Kovács, K. (1972). *Acta Chim. Hung.* **74**, 479–497.
Bernstein, J. (2002). *Polymorphism in Molecular Crystals.* Oxford: Clarendon Press.
Bernstein, J., Davis, R. E., Shimoni, L. & Chang, N.-L. (1995). *Angew. Chem. Int. Ed. Eng.* **34**, 1555–1573.
Enraf–Nonius (1992). *CAD*-4 *Express Manual.* Enraf–Nonius Delft, The Netherlands.
Etter, M. C. (1990). *Acc. Chem. Res.* **23**, 120–126.
Fábián, L. & Kálmán, A. (1999). *Acta Cryst.* B**55**, 1099–1108.
Fábián, L. & Kálmán, A. (2004). *Acta Cryst.* B**60**, 547–588.
Harms, K. (1996). *XCAD*-4. Philipps University of Marburg, Germany.
Jeffrey, G. A. & Saenger, W. (1991). *Hydrogen Bonding in Biological Structures.* Berlin, Heidelberg: Springer Verlag.
Kálmán, A., Argay, Gy., Fábián, L., Bernáth, G. & Fülöp. F. (2001). *Acta Cryst.* B**57**, 539–550.
Kálmán, A., Fábián, L., Argay, Gy., Bernáth, G. & Gyarmati, Zs. (2002*a*). *Acta Cryst.* B**58**, 494–501.
Kálmán, A., Fábián, L., Argay, Gy., Bernáth, G. & Gyarmati, Zs. (2002*b*). *Acta Cryst.* B**58**, 855–863.
Kálmán, A., Fábián, L., Argay, Gy., Bernáth, G. & Gyarmati, Zs. (2003). *J. Am. Chem. Soc.* **125**, 34–35.
Kálmán, A. &. Párkányi, L. (1997). *Adv. Mol. Struct. Res.* **3**, 189–226.
Kálmán, A., Párkányi, L. & Argay, Gy. (1993). *Acta Cryst.* B**49**, 1039–1049.
McCrone, W. C. (1965). *Physics and Chemistry of the Organic Solid State*, edited by D. Fox, M. M. Labes & A. Weissenberg, pp. 725–767. New York: Wiley Interscience.
Merton, R. K. & Barber, E. (2004). *The Travels and Adventures of Serendipity.* Princeton University Press.
Palau, J., Pascual, J. & Ráfols, J. M. (1964). *Bull. Soc. Chim. Fr.* pp. 269–273.
Riddell, F. G., Bernáth, G. & Fülöp, F. (1995). *J. Am. Chem. Soc.* **117**, 2327–2335.
Sheldrick, G. M. (1997*a*). *SHELXS*97. University of Göttingen, Germany.
Sheldrick, G. M. (1997*b*). *SHELXL*97. University of Göttingen, Germany.
Spek, A. L. (1998). *PLATON.* University of Utrecht, The Netherlands.
Yvon, K., Jeitschhko, W. & Parthé, E. (1977). *J. Appl. Cryst.* **10**, 73–74.